

# Stabilization of Palladium-Nanoparticle-Decorated Postsynthesis-Modified Zr-UiO-66 MOF as a Reusable Heterogeneous Catalyst in C–C Coupling Reaction

Leila Mohammadi, Mojtaba Hosseinifard,\* and Mohammad Reza Vaezi\*

Cite This: *ACS Omega* 2023, 8, 8505–8518

Read Online

ACCESS |



Metrics &amp; More

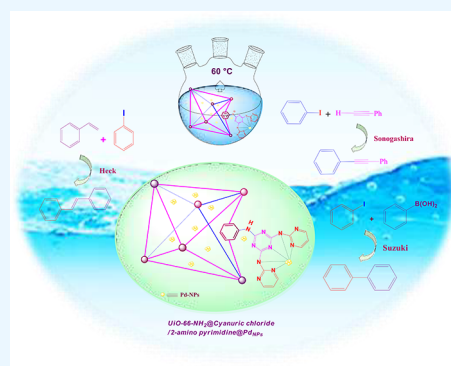


Article Recommendations



Supporting Information

**ABSTRACT:** Here we prepared a highly efficient and reusable catalyst by a step-by-step postsynthesis modification of UiO-66-NH<sub>2</sub> metal–organic frameworks (MOFs) with nitrogen-rich organic ligands and used it as support for the preparation of UiO-66-NH<sub>2</sub>@cyanuric chloride@2-aminopyrimidine/Pd<sub>NPs</sub>. The catalytic performance's results of UiO-66-NH<sub>2</sub>@cyanuric chloride@2-aminopyrimidine/PdNPs, UiO-66-NH<sub>2</sub>/PdNPs, and UiO-66-NH<sub>2</sub>@cyanuric chloride/PdNPs indicate high efficiency of the modulation of the microenvironment of the palladium NPs. The addition of N-rich organic ligands through postsynthesis modification caused a unique structure of the final composite in favor of the progress of the C–C coupling reaction. Various techniques, including FT-IR, XRD, SEM, TEM, EDS, and elemental mapping, were used to characterize UiO-66-NH<sub>2</sub>@cyanuric chloride@2-aminopyrimidine/Pd<sub>NPs</sub>, indicating its successful preparation. Three C–C coupling reactions, including the Suzuki, Heck, and Sonogashira coupling reactions, were promoted using the produced catalyst. As a result of the postsynthesis modification (PSM), the proposed catalyst displays improved catalytic performance. In addition, the suggested catalyst was highly recyclable up to ten times without leaching of PdNPs.



## 1. INTRODUCTION

Cross-couplings and related reactions are considered one of the most challenging and highly efficient synthetic protocols.<sup>1–3</sup> The C–C catalyzed cross-coupling reactions are generally promoted through fundamental transition-metal-catalyzed transformations, in particular, palladium-catalyzed reactions, which are a powerful route to construct carbon–carbon bonds and are currently applicable to the development of the synthesis of functional organic compounds.<sup>4–9</sup> It is noteworthy that synthetic organic chemistry has been expanded via palladium-catalyzed cross-coupling reactions such as Suzuki–Miyaura,<sup>10,11</sup> Sonogashira–Mizorogi,<sup>12</sup> Heck, Negishi,<sup>13</sup> Silence,<sup>14</sup> Kumada,<sup>15,16</sup> and Sonogashira reactions,<sup>17</sup> which have evolved in recent years.<sup>18–21</sup>

The growth of a C–C bond is a consequence of a cross-coupling reaction, defined as the substitution of a heteroatom nucleophile for an alkyl, aryl, or vinyl halide.<sup>22</sup> Multiple aryl derivatives may be made in one go with high selectivity and without the need for an intermediate product isolation.<sup>23–26</sup> Also, cross-coupling reactions are considered as a protagonist, which is specifically utilized in the synthesis of diverse symmetric and asymmetric heteroaryl and biaryl patterns which are essential as vital building structures to provide natural products; pharmaceuticals including important hypertensive, fungicide, antimicrobial, antidiabetic, and analgesic

pharmaceutical structures; the antibiotic vancomycin; and anticancer drugs.<sup>27–29</sup>

The tendency of the metal nanoparticle for aggregation in solvents makes it urgent to use heterogeneous supports for their cost-effective, green, and reusable applications.<sup>30–32</sup> The aggregation of metal NPs decreases their surface area, resulting in diminishing or even quenching of the catalytic activities. Heterogeneous supports not only can prevent aggregation of the NPs but also can boost their catalytic performance or add some new features to the resulting composite.<sup>33–35</sup>

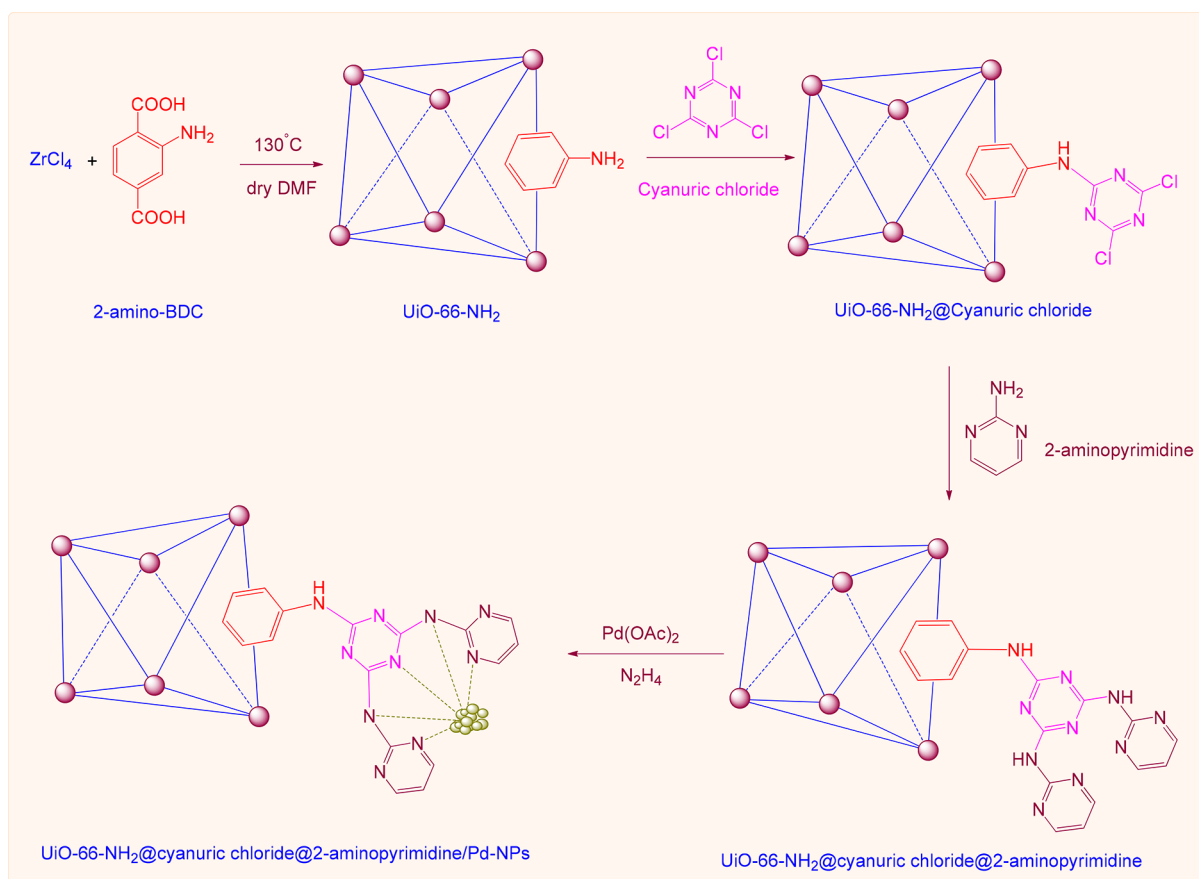
The preparation of organic compounds in green aquatic solvents or solvent-free conditions is a hot topic in today's scientific community.<sup>36,37</sup> Accomplishments within the field of green chemistry have opened up an awesome prospect for more prominent impacts on the efficiency and performance of chemicals and reduced their adverse effects, also facilitating the safety and wellbeing of incorporating mild conditions as well expanding the scope of various organic reactions.<sup>24,38–43</sup>

Received: November 30, 2022

Accepted: February 3, 2023

Published: February 24, 2023



**Scheme 1. Schematic Synthesis of Palladium Nanoparticles Immobilized on UiO-66-NH<sub>2</sub>@Cyanuric Chloride@2-Aminopyrimidine**


One of the most popular materials for the heterogenization of metal NPs is metal–organic frameworks (MOFs), a family of porous materials with tunable chemical and physical properties.<sup>44–46</sup> The designable structure of these materials leads to their broad application in various branches of chemistry, including catalysis, photocatalysis, electrocatalysis, adsorption, separation, drug delivery, and organic transformation.<sup>47–49</sup> Moreover, postsynthesis modification (PSM) allows for the extensive tuning of the chemical and physical characteristics in MOFs by implanting a wide variety of organic and inorganic functionalities.<sup>50–54</sup>

UiO-66-NH<sub>2</sub>, a MOF derived from Zr-terephthalate, which has remarkable chemical, thermal, and mechanical stability and intrinsic open metal sites (OMSs), large surface area, and the presence of the amino group, was an excellent candidate for postfunctionalization. Depending on the application, the organic linker, such as 2-aminopyrimidine, can serve as a binding center to alter the electronic structure of UiO-66-NH<sub>2</sub>.<sup>55–58</sup> In order to synthesize UiO-66-NH<sub>2</sub>, the Zr<sub>6</sub> cluster, [Zr<sub>6</sub>O<sub>4</sub>(OH)<sub>4</sub>], an octahedral secondary building unit (SBU), which is coordinated to 2-amino-1,4-benzenedicarboxylate (BDC) in a 3D 1:12 unit ratio, is responsible for the compound's remarkable stability in aqueous environments.<sup>55</sup> The extraordinary stability of the UiO-66 structure may be attributed to the strong attraction between the negatively charged carboxylic acids and the positively charged Zr<sup>4+</sup> ions, as well as the packed secondary building block (SBU) that prevents H<sub>2</sub>O molecules from reaching the zirconia cluster.<sup>58</sup> There are several reports on the applications of various UiO-66

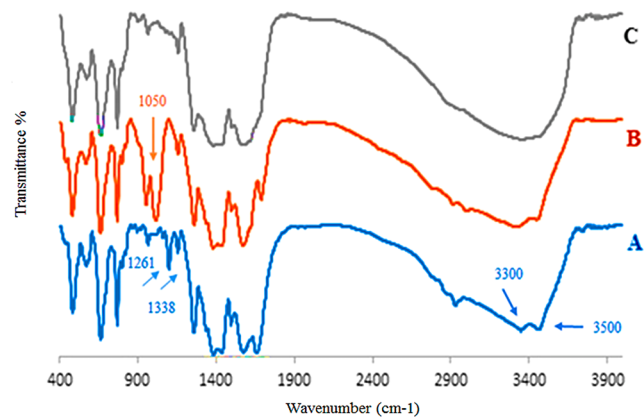


**Figure 1.** IR spectra of (A) UiO-66-NH<sub>2</sub>, (B) UiO-66-NH<sub>2</sub>@cyanuric chloride, and (C) UiO-66-NH<sub>2</sub>@cyanuric chloride@2-aminopyrimidine.

derivatives being synthesized from postimmobilized metal ions or metal nanoparticles. Subsequently, covalent functionalization with 2-aminopyrimidine generated amino moieties in situ. Therefore, 2-aminopyrimidine as a superb N-rich organic ligand persuaded us to utilize it to anchor Pd ions at the outer shell of Zr-UiO-66-NH<sub>2</sub>.<sup>55–58</sup>

Here, we modified the structure of an UiO-66-NH<sub>2</sub> MOF with 2-aminopyrimidine, a N-rich organic compound, using a PSM approach and employed it as support to heterogenize the PdNPs. The manufactured UiO-66-NH<sub>2</sub>@cyanuric chloride/2-aminopyrimidine/Pd<sub>NP</sub> was employed as a catalyst to promote

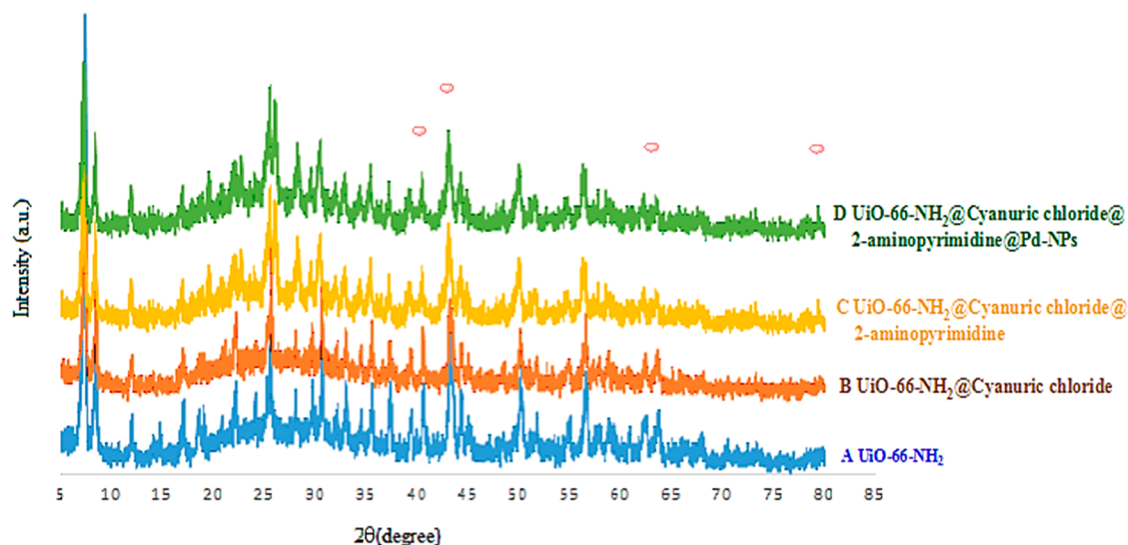


**Figure 2.** Powder XRD spectra patterns of (A) UiO-66-NH<sub>2</sub>, (B) UiO-66-NH<sub>2</sub>@cyanuric chloride, (C) UiO-66-NH<sub>2</sub>@cyanuric chloride@2-aminopyrimidine, and (D) UiO-66-NH<sub>2</sub>@cyanuric chloride@2-aminopyrimidine/Pd<sub>NPs</sub>.

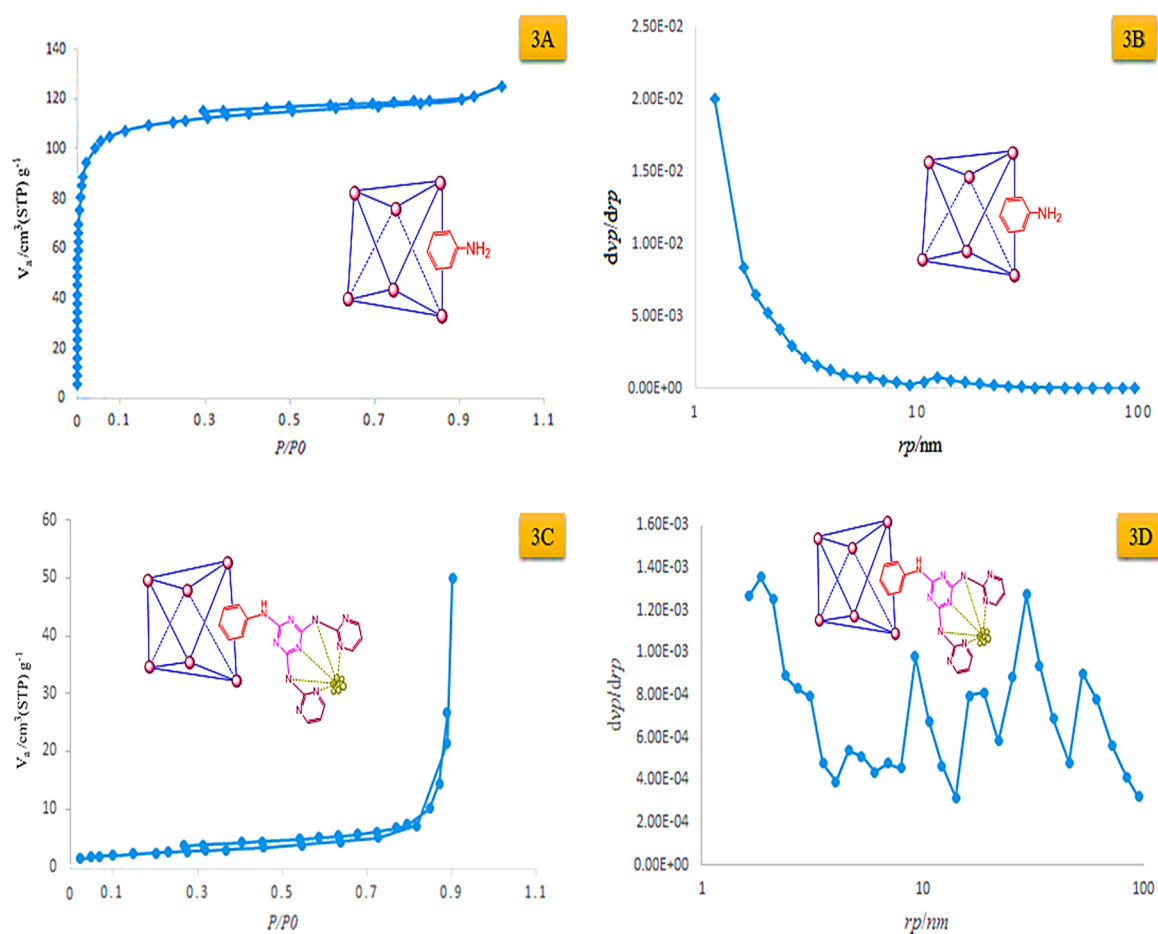


**Figure 3.** (A) BET and (B) BJH of UiO-66-NH<sub>2</sub>. (C) BET and (D) BJH of UiO-66-NH<sub>2</sub>@cyanuric chloride@2-aminopyrimidine.

a series of C–C coupling reactions. The suggested catalyst exhibits increased catalytic performance as a consequence of the PSM. The recommended catalyst was also extremely recyclable for up to eight cycles.

## 2. RESULTS AND DISCUSSION

Following our previous attempts to develop facile and sustainable methodologies for developing various organic reactions, in this report, we introduce a highly efficient and

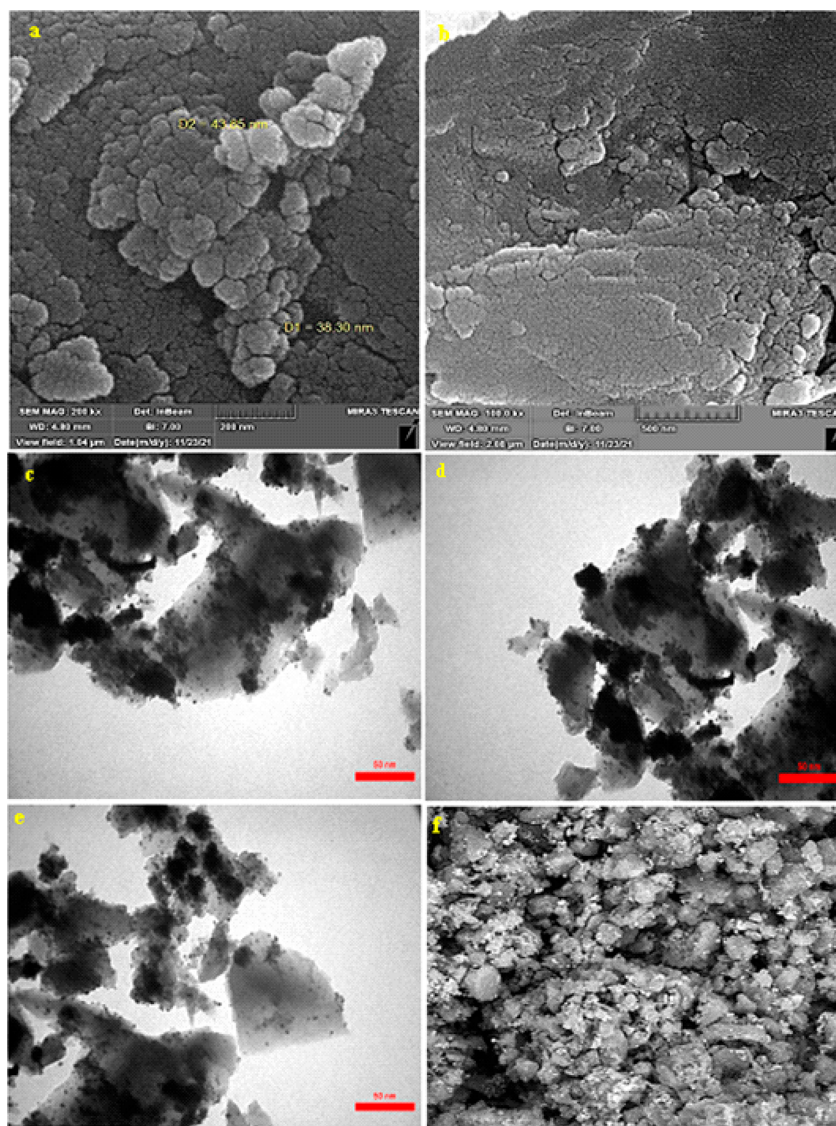


**Figure 4.** (a,b) SEM, (c,d,e) TEM, and (f) STEM of UiO-66-NH<sub>2</sub>@cyanuric chloride@2-aminopyrimidine/Pd<sub>NPs</sub>.

recyclable palladium-based catalyst for the promotion of the C–C coupling reaction. First, UiO-66-NH<sub>2</sub> was prepared and modified with N-rich organic ligands. A step-by-step PSM method was used to introduce the cyanuric chloride and 2-aminopyrimidine to the frameworks. Then, synthesized UiO-66-NH<sub>2</sub>@cyanuric chloride@2-aminopyrimidine was used as a support for the heterogenization of the Pd<sub>NPs</sub> (Scheme 1). Finally, the manufactured UiO-66-NH<sub>2</sub>@cyanuric chloride@2-aminopyrimidine/Pd<sub>NP</sub> was employed as a catalyst for the C–C coupling reaction.

**Fourier Transform Infrared Spectrometer (FT-IR) and X-ray Diffraction (XRD).** The FT-IR spectra of UiO-66-NH<sub>2</sub>, UiO-66-NH<sub>2</sub>@cyanuric chloride, and UiO-66-NH<sub>2</sub>@cyanuric chloride@2-aminopyrimidine are represented in Figure 1. The FT-IR spectra of bare UiO-66-NH<sub>2</sub> (Figure 1A) show broad peaks at 1500–1600 and 3300–3500 cm<sup>-1</sup>, regarding the free and uncoordinated NH<sub>2</sub> groups. Stretching vibrations of the C–N bonding of H<sub>2</sub>BDC–NH<sub>2</sub> show themselves at 1261 and 1338 cm<sup>-1</sup>. The cyanuric-chloride-modified MOF shows less intensity for the broad peak of the NH<sub>2</sub> group at 3300–3500 cm<sup>-1</sup>, indicating less free and available uncoordinated NH<sub>2</sub>. Moreover, a new sharp peak at 1050 cm<sup>-1</sup> appeared, which

indicates the presence of cyanuric chloride in the compound (Figure 1B). The same peak disappears from the IR spectra of the palladium-nanoparticle-immobilized UiO-66-NH<sub>2</sub>@cyanuric chloride@2-aminopyrimidine due to the coordination of 2-aminopyrimidine to the cyanuric chloride (Figure 1C). Other characteristic peaks of various parts of the composite overlapped, and other characterization methods were used to prove the formation of the catalyst.

The crystalline structure of as-synthesized UiO-66-NH<sub>2</sub>, UiO-66-NH<sub>2</sub>@cyanuric chloride, UiO-66-NH<sub>2</sub>@cyanuric chloride@2-aminopyrimidine, and UiO-66-NH<sub>2</sub>@cyanuric chloride@2-aminopyrimidine/Pd<sub>NPs</sub> is investigated by an XRD technique (Figure 2). The XRD pattern of bare UiO-66-NH<sub>2</sub> reveals all the supposed characteristics, which prove its crystallinity and successful synthesis (Figure 2A). The XRD pattern of cyanuric chloride modified UiO-66-NH<sub>2</sub> exhibits no noticeable change in comparison to the bare MOF, which proves that the postsynthesis modification process did not affect the crystallinity (Figure 2B). The XRD pattern of UiO-66-NH<sub>2</sub>@cyanuric chloride@2-aminopyrimidine exhibits minor broadening in the XRD peaks of the MOF, which shows that further modification leads to a minor loss of

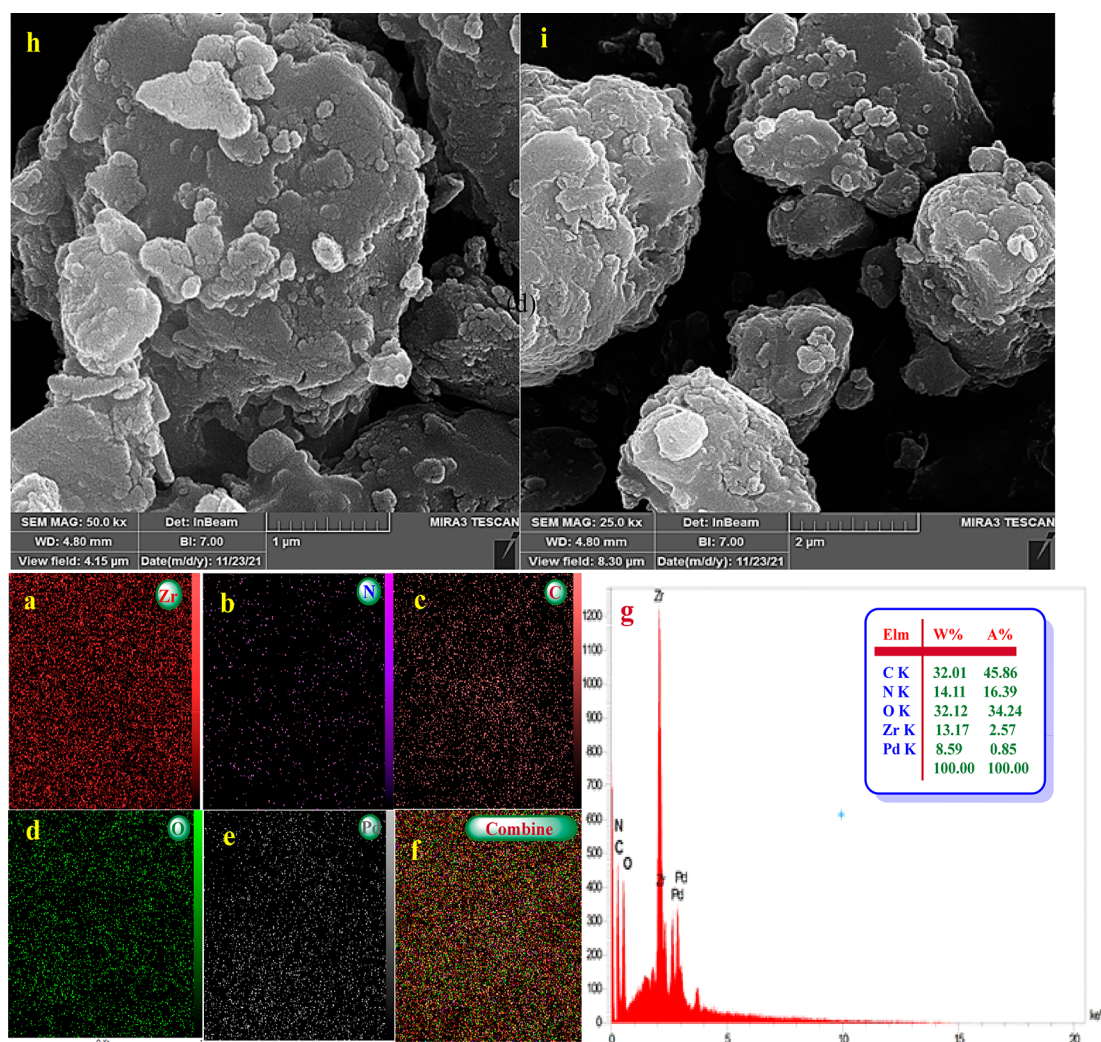


**Figure 5.** (h, i) SEM and (g) EDS spectra of UiO-66-NH<sub>2</sub>@cyanuric chloride@2-aminopyrimidine/Pd<sub>NPs</sub>. EDS mapping of (a) zirconium, (b) nitrogen, (c) carbon, (d) oxygen, (e) palladium, and (f) combined and (g) element percentage table from EDS.

crystallinity, proving the successful modification (Figure 2C). Obviously, the XRD diffraction patterns of UiO-66-NH<sub>2</sub>, UiO-66-NH<sub>2</sub>@cyanuric chloride, UiO-66-NH<sub>2</sub>@cyanuric chloride@2-aminopyrimidine, and UiO-66-NH<sub>2</sub>@cyanuric chloride@2-aminopyrimidine PdNPs, respectively, at  $2\theta = 7.3, 8.7,$  and  $26.1^\circ$ , indicate the preservation of the internal retention based on postsynthesis changes of UiO-66-NH<sub>2</sub>.<sup>29,54</sup> The diffraction peaks associated with UiO-66-NH<sub>2</sub>@cyanuric chloride@2-aminopyrimidine PdNPs correspond to standard Bragg reflections (111), (200), (220), and (311) of the face-centered cubic lattice of Pd<sub>NPs</sub> (Figure 2D).<sup>59</sup> These spectra also exhibit all the characteristics of UiO-66-NH<sub>2</sub>, with a minor shift to higher  $2\theta$  which is a natural result of the composition, proving that the MOF preserves its crystalline structure through the whole synthesis process.

**N<sub>2</sub> Adsorption–Desorption Experiment.** A N<sub>2</sub> adsorption–desorption experiment was conducted for bare and modified UiO-66-NH<sub>2</sub> at 77 K to determine the porosity of the MOF. The Brunauer–Emmett–Teller (BET) method was conducted to calculate the surface area of the samples (Figure 3). The adsorption–desorption isotherm of the bare UiO-66-NH<sub>2</sub> shows a type I isotherm, which suggests the microporosity of its structure, with a surface area of 385 cm<sup>2</sup> g<sup>-1</sup>. The BJH plot of UiO-66-NH<sub>2</sub> confirms the microporosity of

its matrix. This plot shows only one type of micropore in the bare MOF structure with a pore diameter of 1.31 nm (Figure 3C). The modified MOF shows a dramatic decrease in surface area from 385 to 155 cm<sup>2</sup> g<sup>-1</sup>. This result is a consequence of the successful PMS of the MOF, in which the cyanuric chloride and 2-aminopyrimidine filled pores of UiO-66-NH<sub>2</sub> and reduced its surface area (Figure 3B and D).

**Field Emission Scanning Electron Microscopy and Transmission Microscopy Electron.** The morphology and surface structure of UiO-66-NH<sub>2</sub>@cyanuric chloride@2-aminopyrimidine/Pd<sub>NPs</sub> are investigated by SEM and TEM techniques (Figure 4a,b). SEM images show the coarse surface of UiO-66-NH<sub>2</sub> after the postsynthesis modification process, which is a natural result of the PSM and composition with the palladium NPs (Figure 4a). Because of the obtained results from the BET, showing that the pores of the MOF are laden due to the PSM, we try to use the surface of the modified MOF as a stand to load the PdNPs. In this context, we used hydrazine hydrate as a reductant, which results in the formation of bigger NPs compared to other reductants such as NaBH<sub>4</sub>, hoping to form Pd<sub>NPs</sub> over the surface of the modified MOF. The TEM image exhibits the presence of well-dispersed PdNPs over the surface of UiO-66-NH<sub>2</sub> (Figure 4b–d).

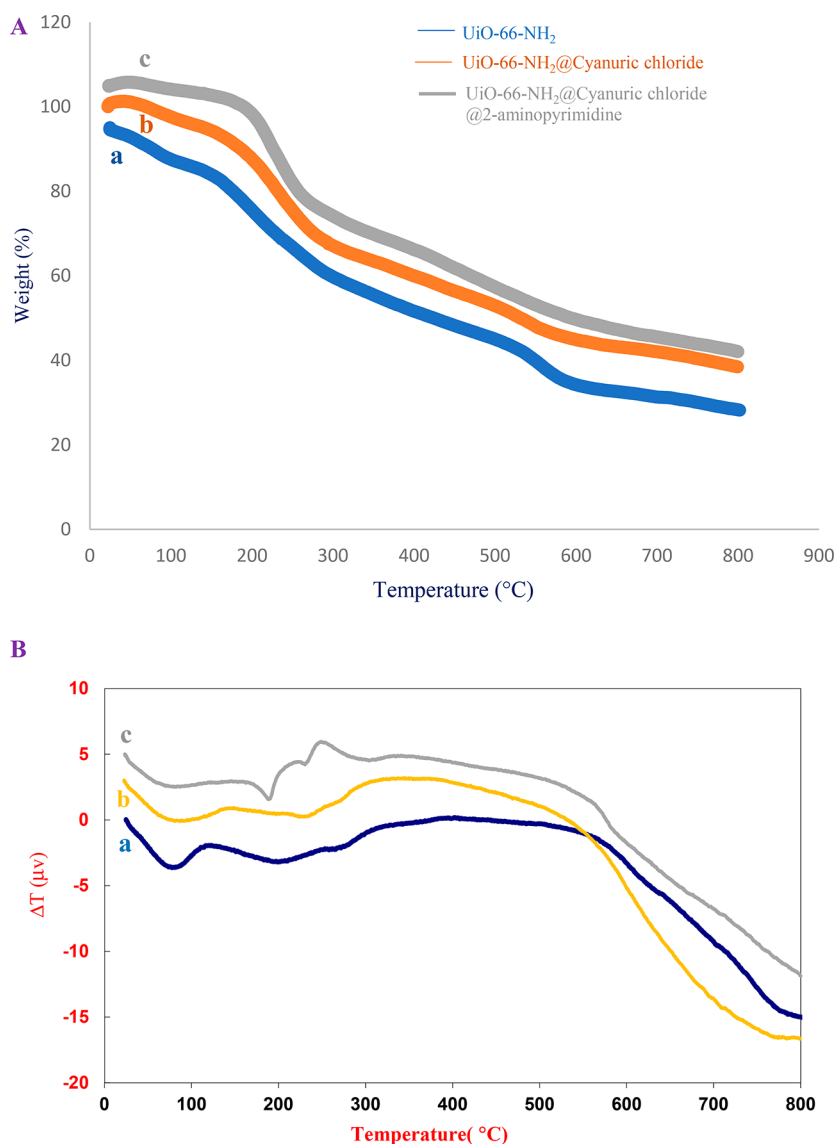


**Figure 6.** (A, B) Comparison of TGA and DTA profiles of (a) UiO-66-NH<sub>2</sub>, (b) UiO-66-NH<sub>2</sub>@cyanuric chloride, and (c) UiO-66-NH<sub>2</sub>@cyanuric chloride@2-aminopyrimidine.

EDS and elemental mapping analysis investigate the elemental composition and spatial distribution of elements in the final composite (Figure 4e and inset images). SEM-EDS analysis confirms the presence of O, C, N, Zr, and Pd in UiO-66-NH<sub>2</sub>@cyanuric chloride@2-aminopyrimidine/Pd<sub>NPs</sub> with an 8.59 wt % loading of palladium NPs, and STEM elemental mapping exhibits uniform elemental dispersion in the sample matrix, proving its successful formation (Figure 5a–i).

**Thermogravimetric Analysis.** The TGA and DTA profiles of UiO-66-NH<sub>2</sub> are represented in Figure 6a. The TGA curve exhibits a two-step weight loss. The first step occurs during the first 280 °C, concerned with the loss of adsorbed gas and coordinated hydroxyl groups to the zirconium cluster. The second step occurs between 280 and 800 °C, ascribed to the destruction of the frameworks. The final residue for the bare UiO-66-NH<sub>2</sub> is 33.18%, which is the remaining zirconium oxide weight. The TGA curves of the UiO-66-NH<sub>2</sub>@cyanuric chloride and UiO-66-NH<sub>2</sub>@cyanuric chloride@2-aminopyrimidine show the same weight loss profile as the UiO-66-NH<sub>2</sub> with the final residue of 38.43%

and 37.03%, respectively, indicating the higher thermal resistance of the modified MOF (Figure 6b and c).

**Catalytic Performance.** After careful characterization of our proposed catalyst, we assess the catalytic application of UiO-66-NH<sub>2</sub>@cyanuric chloride/2-aminopyrimidine/Pd<sub>NPs</sub> for various coupling reactions, including Heck, Sonogashira, and Suzuki. We begin our inquiry by assessing the catalytic efficacy of the proposed catalyst for promoting the Suzuki reaction. The reaction between iodobenzene and phenylboronic acid in the company of UiO-66-NH<sub>2</sub>@cyanuric chloride/2-aminopyrimidine/Pd<sub>NPs</sub> is selected as the template reaction. The effects of the time, temperature, solvent type, base, and amount of catalyst on the reaction rate are studied, and the outcomes are illustrated in Table 1. To determine the optimal solvent, the progress of the Suzuki-coupling reaction of the model reaction in the company of the suggested catalyst in various solvents, including water, toluene, DMSO, DMF, CH<sub>2</sub>Cl<sub>2</sub>, MeCN, a combination of ethanol and water, ethanol, tetrahydrofuran, and NMP, was monitored. This study reveals that ethanol shows the most satisfying outcome. The temperature was raised to 80 °C, and the best results were

Table 1. Findings of the Suzuki Coupling Reaction Optimization Experiments<sup>a</sup>

Entrance	Catalyst (mg)	Solvent	T (°C)	Base	Time (min)	Yield (%)
1	-	EtOH absolute	25	K <sub>2</sub> CO <sub>3</sub>	60	-
2	5	EtOH absolute	80	K <sub>2</sub> CO <sub>3</sub>	60	38
3	10	EtOH:H <sub>2</sub> O (1:1)	80	K <sub>2</sub> CO <sub>3</sub>	60	65
4	25	EtOH:H <sub>2</sub> O (1:1)	80	K <sub>2</sub> CO <sub>3</sub>	60	98
5	30	EtOH:H <sub>2</sub> O (1:1)	80	K <sub>2</sub> CO <sub>3</sub>	60	97
6	25	H <sub>2</sub> O	70	K <sub>2</sub> CO <sub>3</sub>	60	99
7	25	H <sub>2</sub> O	65	K <sub>2</sub> CO <sub>3</sub>	60	99
8	25	H <sub>2</sub> O	60	K <sub>2</sub> CO <sub>3</sub>	60	99
9	25	H <sub>2</sub> O	55	K <sub>2</sub> CO <sub>3</sub>	60	92
10	25	H <sub>2</sub> O	60	KOH	60	90
11	25	H <sub>2</sub> O	60	K <sub>3</sub> PO <sub>4</sub> ·3H <sub>2</sub> O	60	78
12	25	H <sub>2</sub> O	60	CH <sub>3</sub> COONa	60	25
13	25	H <sub>2</sub> O	60	Et <sub>3</sub> N	60	50
14	25	H <sub>2</sub> O	60	Piperidine	60	30
15	25	H <sub>2</sub> O	60	Na <sub>2</sub> CO <sub>3</sub>	60	68
16	25	DMSO	60	K <sub>2</sub> CO <sub>3</sub>	60	-
17	25	DMF	60	K <sub>2</sub> CO <sub>3</sub>	60	35
18	25	1,2-dichloromethane CH <sub>2</sub> Cl <sub>2</sub>	40	K <sub>2</sub> CO <sub>3</sub>	60	35
19	25	MeCN	60	K <sub>2</sub> CO <sub>3</sub>	60	10
20	25	PhCH <sub>3</sub>	60	K <sub>2</sub> CO <sub>3</sub>	60	30
21	25	NMP	60	K <sub>2</sub> CO <sub>3</sub>	60	35
22	25	THF	60	K <sub>2</sub> CO <sub>3</sub>	60	20

<sup>a</sup>Conditions for the chemical reaction: 1 mmol of iodobenzene and 1 mmol of phenylboronic acid.

obtained at 60 °C. A further increase in the temperature did not boost the yield of the reaction. Hiring the TLC technique to track the reaction's progress, we determined that at 60 °C in H<sub>2</sub>O the reaction achieved equilibrium after 60 min. The optimal amount of catalyst was determined by observing the progress of the reaction in the company of varying amounts of catalyst. The results of this study suggested that 25 mg of the proposed catalyst is adequate for the Suzuki reaction to proceed optimally. So, according to these investigations, the highest yields are achieved with 25 mg of UiO-66-NH<sub>2</sub>@cyanuric chloride/2-aminopyrimidine/Pd<sub>NPs</sub> catalyst at 60 °C in H<sub>2</sub>O after 60 min.

The optimization test also was run for the Heck and Sonogashira reactions in the company of the proposed catalyst. Tables S1 and S3 summarize the results of this investigation for the Heck and Sonogashira reactions, respectively. The reaction of iodobenzene and styrene was chosen as the template reaction for the Heck reaction, and the reaction of iodobenzene and phenylacetylene was selected as the template reaction for the Sonogashira reaction. According to this study, using H<sub>2</sub>O as the solvent and K<sub>2</sub>CO<sub>3</sub> as the base in the company of 30 mg of UiO-66-NH<sub>2</sub>@cyanuric chloride/2-aminopyrimidine/Pd<sub>NPs</sub> as the catalyst at 60 °C after 120 min resulted in the best yield for the Heck reaction. The same study indicates that the optimum condition for the progress of the Sonogashira reaction is 20 mg of catalyst in H<sub>2</sub>O in the company of K<sub>2</sub>CO<sub>3</sub> at 50 °C and 20 min of reaction time.

After determining the optimal conditions, we test the generalizability of our proposed technique by synthesizing several biphenyl derivatives from diverse precursors. In this context, several aryl halides and aryl boronic acids interacted in the company of the proposed catalyst and under optimal circumstances. Table 2 provides a summary of this study's findings. The data in this table show that the reaction proceeds with high yields when aryl halides are present. This is true whether the aryl halide is located in the aromatic ring's ortho, meta, or para position. As can be seen in the table below, using an aliphatic halide still produced a high-quality harvest. As demonstrated by its ability to catalyze the Suzuki coupling process in the presence of iodo, bromo, and chloro derivatives of aromatic compounds, the suggested catalyst is highly effective and broadly applicable.

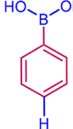
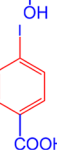
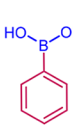
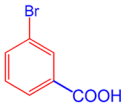
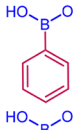
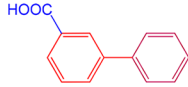
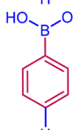
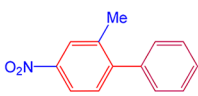
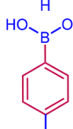
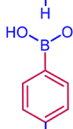
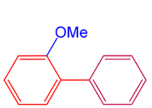
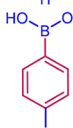
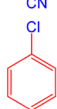
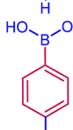
The generality of our proposed method for the Heck and Sonogashira reactions also was conducted, and the outcomes are represented in Tables S2 and S4, respectively. This study indicated that UiO-66-NH<sub>2</sub>@cyanuric chloride/2-aminopyrimidine/Pd<sub>NPs</sub> promote these reactions in good to excellent yields, albeit the yields of some products of the Sonogashira reaction were relatively lower.

**Suggested Mechanism.** Figure 7 indicates a plausible mechanism for the synthesis of the Suzuki coupling reaction using the UiO-66-NH<sub>2</sub>@cyanuric chloride@2-aminopyrimidine@PdNP catalyst. The general mechanism to perform the Suzuki reaction is illustrated through coupling (Ar-X) with an organoboron species (Ar-B(OH)<sub>2</sub>) using catalyst-supported

Table 2. Preparation of Various Organic Compounds by the Suzuki Coupling Reaction under Optimal Conditions<sup>a</sup>

Entry	Aryl halide	Aryl boronic acid	Product	Time (min)	Yield (%)
1				60	97
2				60	97
3				60	99
4				60	99
5				60	99
6				60	77
7				60	92
8				60	95
9				60	99
10				60	98
10				60	99

Table 2. continued

Entry	Aryl halide	Aryl boronic acid	Product	Time (min)	Yield (%)
11				60	92
12				73	99
13				60	76
14				60	95
15				60	90
16				60	98
17				60	96
18				60	98
19				60	97
20				60	95
21				60	94

<sup>a</sup>Conditions for the chemical reaction: 1 mmol of aryl halide, 1 mmol of aryl boronic acid, 60 °C, H<sub>2</sub>O, K<sub>2</sub>CO<sub>3</sub>.

Pd and K<sub>2</sub>CO<sub>3</sub>. First, the oxidative addition of the UiO-66-NH<sub>2</sub>-catalyst-supported Pd to aryl halide occurs to conform aryl-LnPd<sup>+2</sup> species I. Following, in the process of transmetalation, compound II with the boronic acid leads to compound III. Finally, in the last step, reductive elimination occurs, due to creating a carbon–carbon bond to perform IV with concomitant regeneration of L-Pd(0).<sup>60</sup> It is obvious that

the UiO-66-NH<sub>2</sub> with a N-rich organic-ligand-supported Pd catalyst has high catalytic activity for the Suzuki–Miyaura reaction. Owing to their unique N-rich organic ligands through postsynthesis modification of the UiO-66-NH<sub>2</sub> structure, they become a great support as a reservoir to encapsulate the palladium species. The UiO-66-NH<sub>2</sub>-supported Pd catalyst produced by the method of H<sub>2</sub> reduction has high catalytic

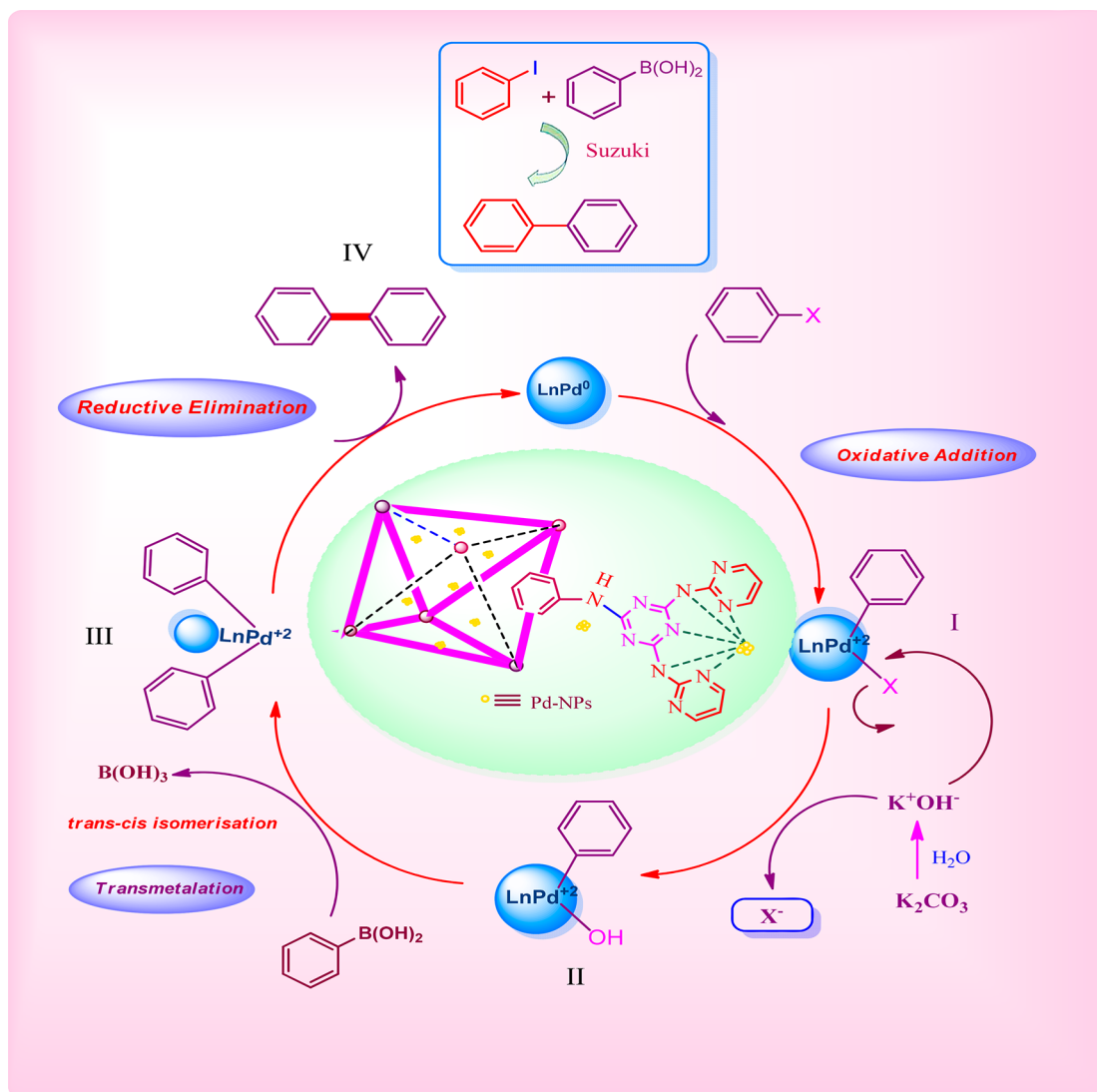


**Figure 7.** Plausible mechanism for synthesis of the Suzuki coupling reaction using UiO-66-NH<sub>2</sub>@cyanuric chloride@2-aminopyrimidine@PdNPs.

activity for the Suzuki–Miyaura reaction and has great potential applications.

The Suzuki cross-coupling reaction catalytic performance of UiO-66-NH<sub>2</sub>@cyanuric chloride/2-aminopyrimidine/Pd<sub>NPs</sub> is compared to some of the published catalysts in the literature in Table 3. According to these data, our suggested catalyst has one of the highest recorded yields. This could result from meticulous postsynthesis alteration using N-rich organic ligands to alter the electrical structure of the UiO-66-NH<sub>2</sub>. The electronic structure of the UiO-66-NH<sub>2</sub> is changed by the addition of 2-aminopyrimidine, which increases the palladium NPs' capacity to catalyze in the finished composite. Also, Tables S6 and S7 indicate that the same trend happens for our proposed catalyst toward the Heck and Sonogashira reactions.

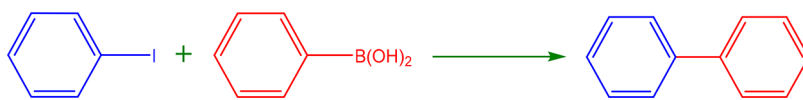
**Recyclability.** The catalyst's reusability is a key feature of its scaled applications because it allows multiple runs of the same reaction. To test how well our proposed catalyst recycles, we filtered it out of the reaction liquid and washed it multiple times with ethyl acetate. We then investigated the effectiveness of the recycled catalyst for the model reaction for a total of ten cycles. As shown in Figure 8, the catalyst's performance did not drop after three cycles; after six runs, it still performed at a level greater than 90% of its initial use. The exceptional reusability

of the proposed catalyst may be attributed to the great water resistance of UiO-66-NH<sub>2</sub> in aquatic environments. Moreover, the PSM of the UiO-66-NH<sub>2</sub> prevents the accessibility of water molecules to the zirconium SBU by filling the pores of the MOF and increasing its stability. As Figure S1 indicates, the UiO-66-NH<sub>2</sub>@cyanuric chloride/2-aminopyrimidine/Pd<sub>NPs</sub> show excellent reusability for the Heck and Sonogashira coupling reactions up to eight cycles.

### 3. CONCLUSIONS

In this study, UiO-66-NH<sub>2</sub> was chosen as a support for the heterogenization of the Pd<sub>NPs</sub> due to its high potential for PSM, surface area, and inherent structural resistance. The PSM of the MOF was carried out by a step-by-step strategy, in which a series of N-rich organic compounds were coordinated to the NH<sub>2</sub> groups of the organic ligand of the MOF. The UiO-66-NH<sub>2</sub>@cyanuric chloride/2-aminopyrimidine/Pd<sub>NPs</sub> was characterized by XRD, SEM, TEM, EDS, and elemental mapping, demonstrating its effective preparation. The resulting catalyst was hired to promote the three C–C coupling reactions, including the Suzuki, Heck, and Sonogashira coupling reactions, which showed superior performance. The results of this study indicate that such high efficiency is a result

Table 3. Comparison of the Catalytic Performance of the Proposed Catalyst with Some Related Reports in the Literature



Entry	Catalyst	Reaction condition	Yield (%)	Time (h)	ref
1	Pd@Mag-MSN (1)	K <sub>2</sub> CO <sub>3</sub> , CH <sub>2</sub> Cl <sub>2</sub> , 80 °C	85	6	61
2	Xerogel g1-MNPs (1)	Na <sub>2</sub> CO <sub>3</sub> , CH <sub>3</sub> OH, 60 °C	99	2	62
3	Pd/NiFe <sub>2</sub> O <sub>4</sub> (0.1)	Na <sub>2</sub> CO <sub>3</sub> , DMF, 90 °C	50	2	63
4	Pd/Fe <sub>3</sub> O <sub>4</sub> (1)	K <sub>2</sub> CO <sub>3</sub> , DME:H <sub>2</sub> O 3:1, reflux	71	24	64
5	C/Co@PNIPAM-PPh <sub>2</sub> -Pd (3)	K <sub>2</sub> CO <sub>3</sub> , toluene:H <sub>2</sub> O 2:1, 85 °C	99	16	65
6	Co@C@Pd (1.1)	Na <sub>2</sub> CO <sub>3</sub> , THF:H <sub>2</sub> O 1:2, 65 °C	96	2	66
7	Pd/Fe <sub>3</sub> O <sub>4</sub> @C (0.3)	K <sub>2</sub> CO <sub>3</sub> , EtOH, reflux	100	1	67
8	Pd@Fe <sub>3</sub> O <sub>4</sub> (0.816)	K <sub>3</sub> PO <sub>4</sub> , CH <sub>3</sub> OH, 40–65 °C	90	18	68
9	Fe <sub>3</sub> O <sub>4</sub> @PUNP <sup>a</sup> -Pd (0.1)	K <sub>2</sub> CO <sub>3</sub> , H <sub>2</sub> O, 90 °C	98	1	69
10	GA-FSNP@Pd (0.28)	K <sub>2</sub> CO <sub>3</sub> , solvent free, 90 °C	92	0.25	70
11	Pd-IPG (0.1)	NaOH, EtOH:H <sub>2</sub> O, 60 °C	99	1	71
12	GO/NHC-Pd (1)	Na <sub>3</sub> PO <sub>4</sub> ·12H <sub>2</sub> O, H <sub>2</sub> O, 100 °C	91.6	6	72
13	PdNPs on polymer (0.08)	K <sub>2</sub> CO <sub>3</sub> , H <sub>2</sub> O, 25–100 °C	83	5	73
14	Pd-HoMOF (0.4)	KOH, DMF, 100 °C	99	1	74
15	(Pd(II)-NHCs) <sub>n</sub> @nSiO <sub>2</sub> (0.27)	K <sub>2</sub> CO <sub>3</sub> , DMF:H <sub>2</sub> O (2:1), 60 °C	97	6 min	75
16	Pd(II)-NiFe <sub>2</sub> O <sub>4</sub> (0.5)	K <sub>2</sub> CO <sub>3</sub> , EtOH:H <sub>2</sub> O, 80 °C	96	3	63
17	GO-CPTMS@Pd-TKHPP (10)	K <sub>2</sub> CO <sub>3</sub> , EtOH:H <sub>2</sub> O, 80 °C	99	15 min	76
18	UiO-66-NH <sub>2</sub> @cyanuric chloride@2-aminopyrimidine@PdNPs (0.025)	H <sub>2</sub> O, K <sub>2</sub> CO <sub>3</sub> , 60 °C	99	60 min	this study

Figure 8. Recyclability of UiO-66-NH<sub>2</sub>@cyanuric chloride@2-aminopyrimidine@Pd<sub>NPs</sub> catalysts.

of the modulation of the microenvironment of the palladium NPs. The proposed catalyst exhibited superior recycling performance due to the inherent resistance of the UiO-66-NH<sub>2</sub> MOF and the induced resistance due to the PSM. Additionally, the proposed catalyst was reusable up to eight times. The important point in using the desired catalyst in aqueous solvent conditions in all three cases is the Suzuki and Sonogashira and Heck reactions in very mild conditions.

#### 4. EXPERIMENTAL SECTION

All the applied materials and reagents in this work were purchased from Merck and Sigma-Aldrich and used without further purification.

**Synthesis of UiO-66-NH<sub>2</sub>.** To synthesize UiO-66-NH<sub>2</sub>, 2.05 g of benzene terephthalic acid (H<sub>2</sub>BDC-NH<sub>2</sub>) was added to a three-neck balloon containing 65 mL of dimethylformamide (DMF) and stirred for 10 min at room temperature. Then, 2.65 g of ZrCl<sub>4</sub> and 55 mL of DMF were added to this solution. This solution was surcharged with 2.5 mL of concentrated HCl as a modulator, and the obtained solution was stirred under reflux conditions and an argon atmosphere at

130 °C for 24 h. Finally, the yellow powder was separated from the reaction medium and washed with DMF and methanol three times. The MOF was activated by soaking the as-synthesized UiO-66-NH<sub>2</sub> in methanol for 3 days and drying under a vacuum at 60 °C.

**Synthesis of UiO-66-NH<sub>2</sub>@Cyanuric Chloride.** Postsynthesis modification of UiO-66-NH<sub>2</sub> was performed through the following procedure. First, 0.6 g of cyanuric chloride was dissolved in 50 mL of dry DMSO at 30 °C. Next, 1 g of UiO-66-NH<sub>2</sub> was added to the obtained solution and stirred for 30 h at 55 °C. The resulting solid was filtered and washed with DMSO for purification.

**Synthesis of UiO-66-NH<sub>2</sub>@Cyanuric Chloride@2-Aminopyrimidine.** The postsynthesis modification procedure was further carried out by modification of UiO-66-NH<sub>2</sub>@cyanuric chloride with 2-aminopyrimidine. To a beaker containing absolute ethanol (20 mL), 1 g of UiO-66-NH<sub>2</sub>@cyanuric chloride was added and stirred for 10 min. To another beaker containing 20 mL of absolute ethanol was added 1 g of 2-aminopyrimidine, and the mixture was stirred until it was completely dissolved. Then, the contents of 2-aminopyrimidine were dissolved in ethanol, added to UiO-66-NH<sub>2</sub>@cyanuric chloride, and stirred for 24 h at 60 °C. Finally, the precipitate was filtered, washed with absolute ethanol, and dried at 45 °C.

**Synthesis and Stabilization of PdNPs.** First, 0.04 g of palladium acetate (Pd(OAc)<sub>2</sub>) was dissolved in 50 mL of acetonitrile at room temperature. Then, 0.2 g of the UiO-66-NH<sub>2</sub>@cyanuric chloride@2-aminopyrimidine was added to the flask containing the transparent amber color solution of palladium acetate in acetonitrile and kept stirring at 40–45 °C for 8 h. Finally, the temperature was lowered to RT, and the reaction mixture was charged with 0.3 mL of freshly prepared hydrazine hydrate solution (3 drops of hydrazine hydrate in 3 mL of deionized water) and kept stirring at RT for another 24 h. Finally, the reaction mixture was separated using a 9000 rpm centrifuge, washed once with acetonitrile, and dried in an oven.

**General Procedure for the Suzuki Reaction.** Typically, 1 mmol of the appropriate aryl halide and 1.1 mmol of the aryl boronic acid were mixed in distilled water ( $\text{H}_2\text{O}$  as a green solvent) (3 mL) in a single-neck flask (10 mL). To this mixture, 0.025 g of the as-prepared UiO-66- $\text{NH}_2$ @cyanuric chloride/2-aminopyrimidine/ $\text{Pd}_{\text{NPs}}$  and 2 mmol of  $\text{K}_2\text{CO}_3$  were added and agitated. The appropriate temperature and time for each reaction vary based on the applied precursor. TLC monitored the progress of the reaction with the solvent ratio (*n*-Hex:EtOAc 7:3). At the end of each reaction, the catalyst was filtered, the mixture cooled to 25 °C, and the organic phase extracted with diethyl acetate. Then it was dried over magnesium sulfate ( $\text{MgSO}_4$ ). After a while,  $\text{MgSO}_4$  was separated by filtration; the organic solvent was evaporated; and column chromatography was hired to purify the products in a solvent ratio of *n*-hexane:ethyl acetate of 1:5. The physical data (melting point), FT-IR, and NMR techniques were used for the identification of the products (Supporting Information).

**General Procedure for the Heck Reaction.** In a suitable round-bottomed flask (10 mL), 1 mmol of the desired aryl halide, 1.1 mmol of olefin, 2 mmol of potassium carbonate ( $\text{K}_2\text{CO}_3$ ), distilled water (3 mL), and 0.03 g of the newly synthesized UiO-66- $\text{NH}_2$ @cyanuric chloride/2-aminopyrimidine/ $\text{Pd}_{\text{NP}}$  catalyst were added at 60 °C. The mixture was centrifuged at the end of the reaction process to separate the catalyst. After cooling the resulting mixture, ethyl acetate was used to extract the products. The organic solvent was evaporated after drying with  $\text{MgSO}_4$ . Column chromatography was hired to purify the products in a solvent ratio of *n*-hexane:ethyl acetate of 1:5. The physical data (melting point), FT-IR, and NMR technique were used for the identification of the products (Supporting Information).

**General Procedure for the Sonogashira Reaction.** Typically, 1.2 mmol of acetylene and 1 mmol of the corresponding halobenzene were mixed in 3 mL of distilled water in a one-neck balloon. Amounts of 20 mg of UiO-66- $\text{NH}_2$ @cyanuric chloride/2-aminopyrimidine/ $\text{Pd}_{\text{NPs}}$  catalyst and 2 mmol of  $\text{K}_2\text{CO}_3$  were added to this mixture, and the temperature was raised to 50 °C and kept stirring for an appropriate time (Table S4). The progression of the reaction was tracked by TLC using an *n*-Hex:EtOAc 8:1 solvent ratio. After the completion of each reaction, the catalyst was filtered, washed with ethanol, and dried at 60 °C for 20 min. The filtered solution was cooled to ambient temperature, and its organic content was extracted with pure diethyl ether ( $\text{Et}_2\text{O}$ ). Column chromatography was hired to purify the products in a solvent ratio of *n*-hexane:ethyl acetate of 1:4. The physical data (melting point), FT-IR, and NMR techniques were used for the identification of the products (Supporting Information).

## ■ ASSOCIATED CONTENT

### Data Availability Statement

All data generated or analyzed during this study are included in this published article (and its Supporting Information files).

### SI Supporting Information

The Supporting Information is available free of charge at <https://pubs.acs.org/doi/10.1021/acsomega.2c07661>.

Tables S1–S7 are associated with results of the optimization studies, preparation of various organic compounds, comparison of the catalytic performance of the proposed catalyst for Sonogashira and Heck reactions, and comparison of the catalysis activity of

the proposed catalyst for the Sonogashira reaction. Figure S1 demonstrates the reusability of the catalyst for (a) Heck and (b) Sonogashira reactions. Spectra of S1–S84 are related to Suzuki derivatives (S1–S43), Heck derivatives (S44–S67), and Sonogashira derivatives (S68–S84) (PDF)

## ■ AUTHOR INFORMATION

### Corresponding Authors

Mojtaba Hosseinfard – Department of Energy, Materials and Energy Research Center, Karaj, Iran; [orcid.org/0000-0003-3770-5963](https://orcid.org/0000-0003-3770-5963); Email: [m.hosseini@merc.ac.ir](mailto:m.hosseini@merc.ac.ir)

Mohammad Reza Vaezi – Department of Nano Technology and Advanced Materials, Materials and Energy Research Center, Karaj, Iran; Email: [m\\_r\\_vaezi@merc.ac.ir](mailto:m_r_vaezi@merc.ac.ir)

### Author

Leila Mohammadi – Department of Nano Technology and Advanced Materials, Materials and Energy Research Center, Karaj, Iran

Complete contact information is available at:

<https://pubs.acs.org/10.1021/acsomega.2c07661>

### Author Contributions

L.M. prepared the final catalyst of the UiO-66- $\text{NH}_2$ @cyanuric chloride/2-aminopyrimidine/ $\text{Pd}_{\text{NPs}}$  catalyst and synthesized and identified the C–C coupling reaction. L.M. collected the manuscript. M.R.V. (supervisor) and M.H. (supervisor) equally edited the paper.

### Notes

The authors declare no competing financial interest.

## ■ ACKNOWLEDGMENTS

The authors would like to thank the Materials and Energy Research Center (Grant No: 9911940) for the financial support of this project.

## ■ REFERENCES

- (1) Ahadi, A.; Rostamnia, S.; Panahi, P.; Wilson, L. D.; Kong, Q.; An, Z.; Shokouhimehr, M. Palladium comprising dicationic bipyridinium supported periodic mesoporous organosilica (PMO): Pd@ Bipy-PMO as an efficient hybrid catalyst for Suzuki–Miyaura cross-coupling reaction in water. *Catal.* **2019**, *9*, 140.
- (2) Rostamnia, S.; Xin, H. Pd (OAc)<sub>2</sub>@ SBA-15/PrEn nanoreactor: a highly active, reusable and selective phosphine-free catalyst for Suzuki–Miyaura cross-coupling reaction in aqueous media. *Appl. Organomet. Chem.* **2013**, *27*, 348–352.
- (3) Iqbal, M. A.; Lu, L.; Mehmood, H.; Hua, R. Biaryl formation via base-promoted direct coupling reactions of arenes with aryl halides. *ACS omega.* **2021**, *6*, 15981–15987.
- (4) Devendar, P.; Qu, R.-Y.; Kang, W.-M.; He, B.; Yang, G.-F. Palladium-catalyzed cross-coupling reactions: a powerful tool for the synthesis of agrochemicals. *J. Agric. Food. Chem.* **2018**, *66*, 8914–8934.
- (5) Dindarloo Inaloo, I.; Majnooni, S.; Eslahi, H.; Esmailpour, M. Nickel (II) nanoparticles immobilized on EDTA-modified Fe<sub>3</sub>O<sub>4</sub>@ SiO<sub>2</sub> nanospheres as efficient and recyclable catalysts for ligand-free Suzuki–Miyaura coupling of aryl carbamates and sulfamates. *ACS omega.* **2020**, *5*, 7406–7417.
- (6) Chatterjee, S.; Bhattacharya, S. K. Size-Dependent Catalytic Activity and Fate of Palladium Nanoparticles in Suzuki–Miyaura Coupling Reactions. *ACS omega.* **2018**, *3*, 12905–12913.
- (7) Halligudra, G.; Paramesh, C. C.; Mudike, R.; Ningegowda, M.; Rangappa, D.; Shivaramu, P. D. PdII on Guanidine-Functionalized

- Fe<sub>3</sub>O<sub>4</sub> Nanoparticles as an Efficient Heterogeneous Catalyst for Suzuki–Miyaura Cross-Coupling and Reduction of Nitroarenes in Aqueous Media. *ACS omega*. **2021**, *6*, 34416–34428.
- (8) Alamgholiloo, H.; Rostamnia, S.; Hassankhani, A.; Khalafy, J.; Baradaran, M. M.; Mahmoudi, G.; Liu, X. Stepwise post-modification immobilization of palladium Schiff-base complex on to the OMS-Cu (BDC) metal–organic framework for Mizoroki-Heck cross-coupling reaction. *Appl. Organomet. Chem.* **2018**, *32*, e4539.
- (9) Rostamnia, S.; Rahmani, T. Ordered mesoporous SBA-15/PrSO<sub>3</sub>Pd and SBA-15/PrSO<sub>3</sub>PdNP as active, reusable and selective phosphine-free catalysts in C–X activation Heck coupling process. *Appl. Organomet. Chem.* **2015**, *29*, 471–474.
- (10) Chatterjee, A.; Ward, T. R. Recent advances in the palladium catalyzed Suzuki–Miyaura cross-coupling reaction in water. *Catal. Lett.* **2016**, *146*, 820–840.
- (11) Taheri Kal Koshvandi, A.; Heravi, M. M.; Momeni, T. Current applications of Suzuki–Miyaura coupling reaction in the total synthesis of natural products: an update. *Appl. Organomet. Chem.* **2018**, *32*, e4210.
- (12) Mohjer, F.; Mofatehnia, P.; Rangraz, Y.; Heravi, M. M. Pd-free, Sonogashira cross-coupling reaction. An update. *J. Organomet. Chem.* **2021**, *936*, 121712.
- (13) Vlaar, T.; Ruijter, E.; Orru, R. V. Recent Advances in Palladium-Catalyzed Cascade Cyclizations. *Adv. Synth. Catal.* **2011**, *353*, 809–841.
- (14) Johansson Seechurn, C. C.; Kitching, M. O.; Colacot, T. J.; Snieckus, V. Palladium-catalyzed cross-coupling: a historical contextual perspective to the 2010 Nobel Prize. *Angew. Chem., Int. Ed.* **2012**, *51*, 5062–5085.
- (15) Heravi, M. M.; Zadsirjan, V.; Hajiabbasi, P.; Hamidi, H. Advances in Kumada–Tamao–Corriu cross-coupling reaction: an update. *Monatsh. Chem.* **2019**, *150*, 535–591.
- (16) Manolikakes, G.; Knochel, P. Radical Catalysis of Kumada Cross-Coupling Reactions Using Functionalized Grignard Reagents. *Angew. Chem., Int. Ed.* **2009**, *48*, 205–209.
- (17) Căta, L.; Terenti, N.; Cociug, C.; Hădăde, N. D.; Grosu, I.; Bucur, C.; Cojocaru, B.; Parvulescu, V. I.; Mazur, M.; Čejka, J. i. Sonogashira Synthesis of New Porous Aromatic Framework-Entrapped Palladium Nanoparticles as Heterogeneous Catalysts for Suzuki–Miyaura Cross-Coupling. *ACS Appl. Mater. Interfaces.* **2022**, *14*, 10428–10437.
- (18) Sarmah, M.; Neog, A. B.; Boruah, P. K.; Das, M. R.; Bharali, P.; Bora, U. Effect of substrates on catalytic activity of biogenic palladium nanoparticles in C–C cross-coupling reactions. *ACS omega*. **2019**, *4*, 3329–3340.
- (19) Dewan, A.; Sarmah, M.; Thakur, A. J.; Bharali, P.; Bora, U. Greener biogenic approach for the synthesis of palladium nanoparticles using papaya peel: An eco-friendly catalyst for C–C coupling reaction. *ACS omega*. **2018**, *3*, 5327–5335.
- (20) Ishida, J.; Nakatsui, M.; Nagata, T.; Kawasaki, H.; Suzuki, T.; Obora, Y. Synthesis and Characterization of N, N-Dimethylformamide-Protected Palladium Nanoparticles and Their Use in the Suzuki–Miyaura Cross-Coupling Reaction. *ACS omega*. **2020**, *5*, 9598–9604.
- (21) Elkanzi, N. A.; Hrichi, H.; Alolayan, R. A.; Derafa, W.; Zahou, F. M.; Bakr, R. B. Synthesis of chalcones derivatives and their biological activities: a review. *ACS omega*. **2022**, *7*, 27769–27786.
- (22) Ali, A.; Ashfaq, M.; Din, Z. U.; Ibrahim, M.; Khalid, M.; Assiri, M. A.; Riaz, A.; Tahir, M. N.; Rodrigues-Filho, E.; Imran, M.; Kuznetsov, A. Synthesis, Structural, and Intriguing Electronic Properties of Symmetrical Bis-Aryl- $\alpha$ ,  $\beta$ -Unsaturated Ketone Derivatives. *ACS omega*. **2022**, *7*, 39294–39309.
- (23) Mahmood, A.; Munir, R.; Zia-ur-Rehman, M.; Javid, N.; Shah, S. J. A.; Noreen, L.; Sindhu, T. A.; Iqbal, J. Synthesis of sulfonamide tethered (hetero) aryl ethylenes as potential inhibitors of P<sub>2</sub>X receptors: a promising way for the treatment of pain and inflammation. *ACS omega*. **2021**, *6*, 25062–25075.
- (24) Pharande, P.; Rashinkar, G.; Pore, D. Cellulose Schiff base-supported Pd (II): An efficient heterogeneous catalyst for Suzuki–Miyaura cross-coupling. *Res. Chem. Intermed.* **2021**, *47*, 4457–4476.
- (25) Biffis, A.; Centomo, P.; Del Zotto, A.; Zecca, M. Pd metal catalysts for cross-couplings and related reactions in the 21st century: a critical review. *Chem. rev.* **2018**, *118*, 2249–2295.
- (26) Nasrollahzadeh, M.; Issaabadi, Z.; Tohidi, M. M.; Mohammad Sajadi, S. Recent progress in application of graphene supported metal nanoparticles in C–C and C–X coupling reactions. *Chem. Rec.* **2018**, *18*, 165–229.
- (27) Martin, R.; Buchwald, S. L. Palladium-catalyzed Suzuki–Miyaura cross-coupling reactions employing dialkylbiaryl phosphine ligands. *Acc. chem. res.* **2008**, *41*, 1461–1473.
- (28) Surana, K.; Chaudhary, B.; Diwaker, M.; Sharma, S. Benzophenone: A ubiquitous scaffold in medicinal chemistry. *MedChemComm.* **2018**, *9*, 1803–1817.
- (29) Veisi, H.; Abrifam, M.; Kamangar, S. A.; Pirhayati, M.; Saremi, S. G.; Noroozi, M.; Tamoradi, T.; Karmakar, B. Pd immobilization biguanidine modified Zr–UiO-66 MOF as a reusable heterogeneous catalyst in Suzuki–Miyaura coupling. *Sci. Rep.* **2021**, *11*, 1–14.
- (30) Li, S.; He, J.; Xu, Q.-H. Aggregation of metal-nanoparticle-induced fluorescence enhancement and its application in sensing. *ACS omega*. **2020**, *5*, 41–48.
- (31) Yang, Q.; Xu, Q.; Jiang, H.-L. Metal–organic frameworks meet metal nanoparticles: synergistic effect for enhanced catalysis. *Chem. Soc. Rev.* **2017**, *46*, 4774–4808.
- (32) Sadeghi, S. H.; Yaghoobi, M.; Ghasemzadeh, M. A. Synthesis of pyrido [2, 3-d: 5, 6-d'] dipyrimidines using CuFe<sub>2</sub>O<sub>4</sub>/KCC-1/PMA as a novel and efficient nanocatalyst under solvent-free conditions. *Appl. Organomet. Chem.* **2022**, *36*, e6771.
- (33) Diler, F.; Burhan, H.; Genc, H.; Kuyuldar, E.; Zengin, M.; Cellat, K.; Sen, F. Efficient preparation and application of monodisperse palladium loaded graphene oxide as a reusable and effective heterogeneous catalyst for suzuki cross-coupling reaction. *J. Mol. Liq.* **2020**, *298*, 111967.
- (34) Maleki, A.; Taheri-Ledari, R.; Ghalavand, R. Design and fabrication of a magnetite-based polymer-supported hybrid nanocomposite: a promising heterogeneous catalytic system utilized in known palladium-assisted coupling reactions. *Comb. Chem. High Throughput Screen.* **2020**, *23*, 119–125.
- (35) Liu, Q. X.; Zhang, W.; Zhao, X. J.; Zhao, Z. X.; Shi, M. C.; Wang, X. G. NHC PdII Complex Bearing 1, 6-Hexylene Linker: Synthesis and Catalytic Activity in the Suzuki–Miyaura and Heck–Mizoroki Reactions. *Eur. J. Org. Chem.* **2013**, *2013*, 1253–1261.
- (36) Newman, S. G.; Jensen, K. F. The role of flow in green chemistry and engineering. *Green chem.* **2013**, *15*, 1456–1472.
- (37) Polshettiwar, V.; Len, C.; Fihri, A. Silica-supported palladium: Sustainable catalysts for cross-coupling reactions. *Coord. Chem. Rev.* **2009**, *253*, 2599–2626.
- (38) Pálincó, I. Heterogeneous catalysis: A fundamental pillar of sustainable synthesis. In *Green Chemistry*; Elsevier: 2018; pp 415–447.
- (39) Baran, T.; Sargin, I.; Kaya, M.; Menteş, A. An environmental catalyst derived from biological waste materials for green synthesis of biaryls via Suzuki coupling reactions. *J. Mol. Catal. A: Chem.* **2016**, *420*, 216–221.
- (40) Boruah, P. R.; Gehlot, P. S.; Kumar, A.; Sarma, D. Palladium immobilized on the surface of MMT K 10 with the aid of [BMIM][BF<sub>4</sub>]: An efficient catalyst for Suzuki–Miyaura cross-coupling reactions. *Mol. Catal.* **2018**, *461*, 54–59.
- (41) Naeimi, H.; Moradian, M. Copper (I)-N<sub>2</sub>S<sub>2</sub>-salen type complex covalently anchored onto MCM-41 silica: an efficient and reusable catalyst for the A<sub>3</sub>-coupling reaction toward propargylamines. *Appl. Organomet. Chem.* **2013**, *27*, 300–306.
- (42) Terra, J. C.; Moores, A.; Moura, F. C. Amine-functionalized mesoporous silica as a support for on-demand release of copper in the A<sub>3</sub>-coupling reaction: ultralow concentration catalysis and confinement effect. *ACS Sustain. Chem. Eng.* **2019**, *7*, 8696–8705.

- (43) Saneinezhad, S.; Mohammadi, L.; Zadsirjan, V.; Bamoharram, F. F.; Heravi, M. M. Silver nanoparticles-decorated Preyssler functionalized cellulose biocomposite as a novel and efficient catalyst for the synthesis of 2-amino-4H-pyrans and spirochromenes. *Sci. Rep.* **2020**, *10*, 1–26.
- (44) Bagchi, D.; Bhattacharya, A.; Dutta, T.; Nag, S.; Wulferding, D.; Lemmens, P.; Pal, S. K. Nano MOF entrapping hydrophobic photosensitizer for dual-stimuli-responsive unprecedented therapeutic action against drug-resistant bacteria. *ACS Appl. Bio Mater.* **2019**, *2*, 1772–1780.
- (45) Sarker, M.; Shin, S.; Jhung, S. H. Synthesis and functionalization of porous Zr-diaminostilbenedicarboxylate metal–organic framework for storage and stable delivery of ibuprofen. *ACS omega.* **2019**, *4*, 9860–9867.
- (46) Nasrollahzadeh, M.; Issaabadi, Z.; Varma, R. S. Magnetic lignosulfonate-supported Pd complex: renewable resource-derived catalyst for aqueous Suzuki–Miyaura reaction. *ACS omega.* **2019**, *4*, 14234–14241.
- (47) Ghosh, S.; Das, A.; Biswas, S. A functionalized UiO-66 MOF acting as a luminescent chemosensor for selective and sensitive turn-on detection of superoxide and acetylacetone. *MICROPOR MESOPOR MAT.* **2021**, *323*, 111251.
- (48) Kumari, A.; Kaushal, S.; Singh, P. P. Bimetallic metal organic frameworks heterogeneous catalysts: Design, construction, and applications. *Mater. Today Energy.* **2021**, *20*, 100667.
- (49) Liu, J.; Huang, J.; Zhang, L.; Lei, J. Multifunctional metal–organic framework heterostructures for enhanced cancer therapy. *Chem. Soc. Rev.* **2021**, *50*, 1188–1218.
- (50) Rojas, S.; Rodríguez-Diéguez, A.; Horcajada, P. Metal–Organic Frameworks in Agriculture. *ACS Appl. Mater. Interfaces.* **2022**, *14*, 16983–17007.
- (51) Carrillo-Carrión, C. Nanoscale metal–organic frameworks as key players in the context of drug delivery: evolution toward theranostic platforms. *Anal. Bioanal. Chem.* **2020**, *412*, 37–54.
- (52) Yang, J.; Wu, Y.; Wu, X.; Liu, W.; Wang, Y.; Wang, J. An N-heterocyclic carbene-functionalised covalent organic framework with atomically dispersed palladium for coupling reactions under mild conditions. *Green Chem.* **2019**, *21*, 5267–5273.
- (53) Feizi Mohazzab, B.; Jaleh, B.; Issaabadi, Z.; Nasrollahzadeh, M.; Varma, R. S. Stainless steel mesh-GO/Pd NPs: catalytic applications of Suzuki–Miyaura and Stille coupling reactions in eco-friendly media. *Green Chem.* **2019**, *21*, 3319–3327.
- (54) Abánades Lázaro, I.; Wells, C. J.; Forgan, R. S. Multivariate modulation of the Zr MOF UiO-66 for defect-controlled combination anticancer drug delivery. *Angew. Chem.* **2020**, *132*, S249–S255.
- (55) Yuan, S.; Qin, J.-S.; Lollar, C. T.; Zhou, H.-C. Stable metal–organic frameworks with group 4 metals: current status and trends. *ACS cent. sci.* **2018**, *4*, 440–450.
- (56) Wang, Q.; Astruc, D. State of the art and prospects in metal–organic framework (MOF)-based and MOF-derived nanocatalysis. *Chem. rev.* **2020**, *120*, 1438–1511.
- (57) Stock, N.; Biswas, S. Synthesis of metal-organic frameworks (MOFs): routes to various MOF topologies, morphologies, and composites. *Chem. Rev.* **2012**, *112* (2), 933–969.
- (58) Bai, Y.; Dou, Y.; Xie, L.-H.; Rutledge, W.; Li, J.-R.; Zhou, H.-C. Zr-based metal–organic frameworks: design, synthesis, structure, and applications. *Chem. Soc. Rev.* **2016**, *45*, 2327–2367.
- (59) Devi Priya, D.; Athira, C. C.; Mohana Roopan, S. Surface area-enhanced flower-shaped hair protein-supported palladium nanoparticles as sono-photocatalyst towards carbon–carbon bond forming reaction. *Appl. Organomet. Chem.* **2022**, *36*, e6655.
- (60) Joshi, C.; Macharia, J. M.; Izzo, J. A.; Wambua, V.; Kim, S.; Hirschi, J. S.; Vetticatt, M. J. Isotope Effects Reveal the Catalytic Mechanism of the Archetypical Suzuki–Miyaura Reaction. *ACS Catal.* **2022**, *12*, 2959–2966.
- (61) Shaw, B. L. Highly active, stable, catalysts for the Heck reaction; further suggestions on the mechanism. *Chem. Commun.* **1998**, *13*, 1361–1362.
- (62) Liao, Y.; He, L.; Huang, J.; Zhang, J.; Zhuang, L.; Shen, H.; Su, C.-Y. Magnetite nanoparticle-supported coordination polymer nanofibers: synthesis and catalytic application in Suzuki–Miyaura coupling. *ACS Appl. Mater. Interfaces.* **2010**, *2*, 2333–2338.
- (63) Borhade, S. R.; Waghmode, S. B. Studies on Pd/NiFe<sub>2</sub>O<sub>4</sub> catalyzed ligand-free Suzuki reaction in aqueous phase: synthesis of biaryls, terphenyls and polyaryls. *Beilstein J. Org. Chem.* **2011**, *7*, 310–319.
- (64) Elazab, H. A.; Siamaki, A. R.; Moussa, S.; Gupton, B. F.; El-Shall, M. S. Highly efficient and magnetically recyclable graphene-supported Pd/Fe<sub>3</sub>O<sub>4</sub> nanoparticle catalysts for Suzuki and Heck cross-coupling reactions. *Appl. Catal. A: Gen.* **2015**, *491*, 58–69.
- (65) Zeltner, M.; Schätz, A.; Hefti, M. L.; Stark, W. J. Magneto-thermally responsive C/Co@PNIPAM-nanoparticles enable preparation of self-separating phase-switching palladium catalysts. *J. Mater. Chem.* **2011**, *21*, 2991–2996.
- (66) Faisal, S. *ROMP-Derived Alkylating Reagents and Scavengers: Application in Library Development and Sequestration*; University of Kansas, 2016.
- (67) Li, R.; Zhang, P.; Huang, Y.; Zhang, P.; Zhong, H.; Chen, Q. Pd–Fe<sub>3</sub>O<sub>4</sub>@C hybrid nanoparticles: preparation, characterization, and their high catalytic activity toward Suzuki coupling reactions. *J. Mater. Chem.* **2012**, *22*, 22750–22755.
- (68) Amali, A. J.; Rana, R. K. Stabilisation of Pd (0) on surface functionalised Fe<sub>3</sub>O<sub>4</sub> nanoparticles: magnetically recoverable and stable recyclable catalyst for hydrogenation and Suzuki–Miyaura reactions. *Green Chem.* **2009**, *11*, 1781–1786.
- (69) Yang, J.; Wang, D.; Liu, W.; Zhang, X.; Bian, F.; Yu, W. Palladium supported on a magnetic microgel: an efficient and recyclable catalyst for Suzuki and Heck reactions in water. *Green chem.* **2013**, *15*, 3429–3437.
- (70) Tanhaei, M.; Mahjoub, A.; Nejat, R. Three-Dimensional Graphene–Magnetic Palladium Nanohybrid: A Highly Efficient and Reusable Catalyst for Promoting Organic Reactions. *Catal. Lett.* **2018**, *148*, 1549–1561.
- (71) Kwon, T. H.; Cho, K. Y.; Baek, K.-Y.; Yoon, H. G.; Kim, B. M. Recyclable palladium–graphene nanocomposite catalysts containing ionic polymers: efficient Suzuki coupling reactions. *RSC adv.* **2017**, *7*, 11684–11690.
- (72) Park, J. H.; Raza, F.; Jeon, S.-J.; Kim, H.-I.; Kang, T. W.; Yim, D.; Kim, J.-H. Recyclable N-heterocyclic carbene/palladium catalyst on graphene oxide for the aqueous-phase Suzuki reaction. *Tetrahedron Lett.* **2014**, *55*, 3426–3430.
- (73) Wang, Z. J.; Ghasimi, S.; Landfester, K.; Zhang, K. A. Photocatalytic Suzuki coupling reaction using conjugated microporous polymer with immobilized palladium nanoparticles under visible light. *Chem. Mater.* **2015**, *27*, 1921–1924.
- (74) Dong, D.; Li, Z.; Liu, D.; Yu, N.; Zhao, H.; Chen, H.; Liu, J.; Liu, D. Postsynthetic modification of single Pd sites into uncoordinated polypyridine groups of a MOF as the highly efficient catalyst for Heck and Suzuki reactions. *New J. Chem.* **2018**, *42*, 9317–9323.
- (75) Singh, R.; Sindhu, J.; Devi, M.; Kumar, A.; Kumar, R.; Hussain, K.; Kumar, P. Solid-Supported Materials-Based Synthesis of 2-Substituted Benzothiazoles: Recent Developments and Sanguine Future. *ChemistrySelect.* **2021**, *6*, 6388–6449.
- (76) Bahrami, K.; Kamrani, S. N. Synthesis, characterization and application of graphene palladium porphyrin as a nanocatalyst for the coupling reactions such as: Suzuki–Miyaura and Mizoroki–Heck. *Appl. Organomet. Chem.* **2018**, *32*, e4102.